Journal of the Serbian Chemical Society
JSCS-info@shd.org.rs • www.shd.org.rs/JSCS
J. Serb. Chem. Soc. 81 (9) 979–997 (2016)
JSCS–4902
UDC 547.756+542.9+547.571'551:66.093.1:517.9
Original scientific paper

Solvatochromism of isatin based Schiff bases: An LSER and LFER study

DOMINIK R. BRKIĆ[1], ALEKSANDRA R. BOŽIĆ[1], VESNA D. NIKOLIĆ[2], ALEKSANDAR D. MARINKOVIĆ[3#], HANA ELSHAFLU[3], JASMINA B. NIKOLIĆ[3#*] and SAŠA Ž. DRMANIĆ[3#]

[1]*Belgrade Polytechnic, Brankova 17, 11000 Belgrade, Serbia,* [2]*Faculty of Chemistry, University of Belgrade, Studentski trg 12–16, 11000 Belgrade, Serbia and* [3]*Department of Organic Chemistry, Faculty of Technology and Metallurgy, University of Belgrade, Karnegijeva 4, 11120 Belgrade, Serbia*

(Received 19 January, revised 20 April, accepted 8 May 2016)

Abstract: The derivatives of isatin (1*H*-indole-2,3-dione) have already been reported to show a variety of biological activities. However, there have hitherto been no reports on the solvatochromic effects of isatin derivatives, and it could be of interest to study and relate them to their electronic structures, as a part of the characterisation of these compounds. Linear solvation energy relationships (LSER) were used to analyze the influence of the solvent on the shifts of the UV absorption maxima of investigated isatin derivatives, *i.e.*, isatin based Schiff bases, using Kamlet–Taft model. Linear free energy relationships (LFER) were applied to the substituent-induced NMR chemical shifts (*SCS*) using a single substituent parameter (SSP). The obtained correlations together with theoretical calculations gave insight into the influence of the molecular conformation on the transmission of substituent effects, as well as on solute–solvent interactions. The molecular electrostatic potential (*MEP*) surface map was plotted over the optimized geometry of the molecules in order to visualize the electron density distribution and explain the origin of the solvent––solute interactions.

Keywords: Schiff bases; isatin; LSER; LFER; Kamlet–Taft equation.

INTRODUCTION

Isatin (1*H*-indole-2,3-dione) and its metabolites are components of many natural substances. Isatin is also an integral part of many synthetic compounds used in medicine that display a wide range of activities, such as antiviral, anti-cancer, antibacterial, antituberculosis, antifungal and anticonvulsant. Derivatives

* Corresponding author. E-mail: jasmina@tmf.bg.ac.rs
# Serbian Chemical Society member.
doi: 10.2298/JSC160119049B

of isatin have a special distribution in the brain, peripheral tissues, body fluids as well as specific places where they bind.[1] The most prominent isatin effect is the blocking of other substances and drugs, which has been the subject of a lot of research and has been experimentally confirmed many times. Knowledge about the function and locations of isatin action have resulted in the development of new pharmacological agents that simulate or retard its activity.[1] Recently, a published study on the antimicrobial activity of isatin derivatives, performed by the agar dilution method, against selected strains of bacteria and one fungus, as well as on their antioxidative activity, showed that the examined isatin derivatives possessed moderate to significant activity.[2]

Derivatives of isatin, as well as of its Schiff and Mannich bases, have already been reported to show a variety of biological activities, such as antibacterial,[3] antifungal[4] and anti-HIV activities.[5,6] However, to the best of our knowledge, there have hitherto been no reports on the solvatochromic effects of isatin derivatives.

Absorption spectra in different solvents can be used for investigating the solvatochromic effect of organic molecules. When absorption spectra are measured in solvents of different polarity, it is found that the positions, intensities, and shape of absorption bands are usually influenced by the solvent. These changes are the result of physical intermolecular solute–solvent interaction forces (such as ion–dipole, dipole–dipole, dipole-induced dipole, hydrogen bonding, *etc.*), which above all tend to change the energy difference between the ground and excited state of the chromophore-containing absorption species. The mostly used spectra that can provide information about solute–solvent interactions are: UV–Vis, IR, and ^{1}H- and ^{13}C-NMR spectra.[7]

The UV–Vis and NMR data in the present study were analyzed using linear solvation energy relationships (LSER) and linear free energy relationships (LFER) models, in order to evaluate the influence of solvent–solute interactions and substituent effects, respectively. Quantification of the solvent effects: dipolarity/polarizability and hydrogen-bonding ability on the UV spectral shifts, *i.e.*, ν_{max}, were interpreted by means of the Kamlet–Taft LSER,[8] Eq. (1):

$$\nu_{max} = \nu_0 + s\pi^* + a\alpha + b\beta \quad (1)$$

where ν_{max} is a substituent-dependent value, *i.e.*, absorption frequency, π^* is an index of the solvent dipolarity/polarizability; α is a measure of the solvent hydrogen-bond donor (HBD) acidity; β is a measure of the solvent bond acceptor (HBA) basicity and ν_0 is the regression value in cyclohexane as the reference solvent. The solvent parameters used in Eq. (1) are given in Table S-I of the Supplementary material to this paper. The regression coefficients, s, a and b in Eq. (1), measure the relative susceptibilities of the absorption frequencies to the indicated solvent parameters. The correlations of the absorption frequencies ν_{max}

were determined by means of multiple linear regression analysis, and all correlations fitted at the 95 % confidence level.

In the second part of the work, LFER analysis was applied to the UV and NMR data of the studied compounds (Fig. 1). The transmission of substituent effects from substituent (X) to the carbon atoms of interest were studied using Eq. (2):

$$s = \rho\sigma + h \tag{2}$$

where s is the substituent-dependent value, *i.e.*, substituent induced chemical shift (*SCS*) or absorption frequency (ν); ρ is a proportionality constant (reaction constant) reflecting the sensitivity of the spectral data to the substituent effects; σ is the substituent constant, and h is the intercept (*i.e.*, it describes the unsubstituted member of the series).[9–11] The single substituent parameter (SSP; the Hammett Equation, Eq. (2)) attributes the observed substituent effect to an additive blend of polar and π-delocalization effects given as the corresponding σ value. The transmission of substituent effects, *i.e.*, LFER study, is discussed in relation to the geometry of molecules obtained optimized by DFT calculations.

EXPERIMENTAL

A series of eleven isatin derivatives (1,3-dihydro-3-arylimino-2*H*-indol-2-one) were synthesized by the reaction of isatin and the appropriate aryl amine, presented in Fig. 1. All chemicals used for synthesis were of *p.a.* quality and solvents used for recording UV spectra were of spectrophotometric grade (Sigma–Aldrich). A list of the synthesized compounds is given in Table I.

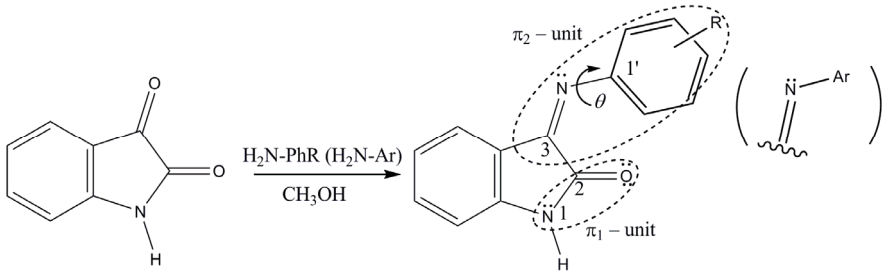

Fig. 1. The chemical synthesis of isatin derivatives with labelling of the π-electronic units

General method for preparation and purification procedure for the synthesized isatin derivatives are described in detail in the Supplementary material. Yields, melting points, ^{1}H- and ^{13}C-NMR analysis, and FTIR data of the obtained isatin derivatives are given in Table S-II of the Supplementary material. Numbering of the atoms used in the NMR analysis is given in Fig. S-1, and examples of the ^{1}H- and ^{13}C-NMR spectra for compound **9** are given in Figs. S-2 and S-3, respectively, all in Supplementary material.

The UV absorption spectra were recorded in the range from 200 to 600 nm in twenty two solvents of different polarity using a Shimadzu 1700A UV–Vis spectrophotometer. Spectra were recorded at 25 °C, in order to study the substituent effect on the solvatochromism of the investigated compounds. The concentration of the derivatives was 1.00×10^{-5} mol dm^{-3}.

TABLE I. A list of synthesized isatin derivatives

Compd.	Compound	Substituent R	Abbreviation
1	1,3-Dihydro-3-(phenylimino)--2*H*-indol-2-one	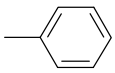	Ph
2	1,3-Dihydro-3-[(2-bromophenyl)imino]-2*H*-indol-2-one	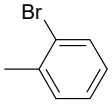	
3	1,3-Dihydro-3-[(3-bromophenyl)imino]-2*H*-indol-2-one	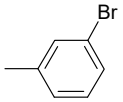	
4	1,3-Dihydro-3-[(4-bromophenyl)imino]-2*H*-indol-2-one	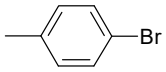	
5	1,3-Dihydro-3-[(3-methyl-2-pyridinyl)imino]-2*H*-indol-2-one	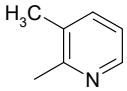	3-Me-2-pyridyl
6	1,3-Dihydro-3-[(4-methyl-2-pyridinyl)imino]-2*H*-indol-2-one	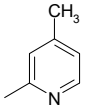	4-Me-2-pyridyl
7	1,3-Dihydro-3-[(5-methyl-2-pyridinyl)imino]-2*H*-indol-2-one	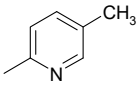	5-Me-2-pyridyl
8	1,3-Dihydro-3-[(6-methyl-2-pyridinyl)imino]-2*H*-indol-2-one	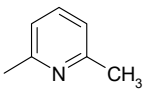	6-Me-2-pyridyl
9	1,3-Dihydro-3-(3-quinolinylimino)-2*H*-indol-2-one	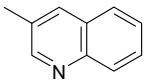	3-Quinolinyl
10	1,3-Dihydro-3-(6-quinolinylimino)-2*H*-indol-2-one	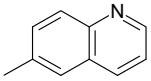	6-Quinolinyl
11	1,3-Dihydro-3-[(8-hydroxy-2--quinolinyl)imino]-2*H*-indol--2-one	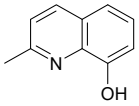	8-OH-2-quinolinyl

Ab initio *theoretical calculation method*

The ground state geometries of compounds **1**–**11** were fully optimized with the DFT method, more specifically, the Becke three-parameter exchange functional (B3) and the Lee–Yang–Parr correlation functional (LYP) with the 6-311G(d,p) basis set without symmetry constraint, and with default tight convergence criteria. The harmonic vibrational frequencies were evaluated at the same level to confirm the nature of the stationary points found; global minima were found for each optimized compound. The theoretical absorption spectra of compound **1** (data shown in the Supplementary material, Table S-VI) were calculated in acetone, acetonitrile, ethanol, tetrahydrofuran, dimethyl sulfoxide, formamide and toluene by the

TD-DFT method using the CAM-B3LYP long range corrected functional[12] and the 6-311G(d,p) basis set. For TD-DFT calculations, the solvents were simulated with the standard polarized continuum model (PCM).[13] All quantum chemical calculations were realised within the Gaussian 09[14] program package. Maps of the molecular electrostatic potential (*MEP*) surface were plotted in the gOpenMol program.[15]

RESULTS AND DISCUSSION

Absorption spectra of the isatin derivatives **1**–**11**, recorded in twenty two solvents, indicate the presence of two bands in the region 200–600 nm corresponding to different electronic transition of investigated compounds. As example of the UV–Vis absorption spectra of compounds **1**–**11** in acetone, acetonitrile (ACN), benzyl alcohol (BnOH) and *N,N*-dimethylformamide (DMF) are given in Fig. 2.

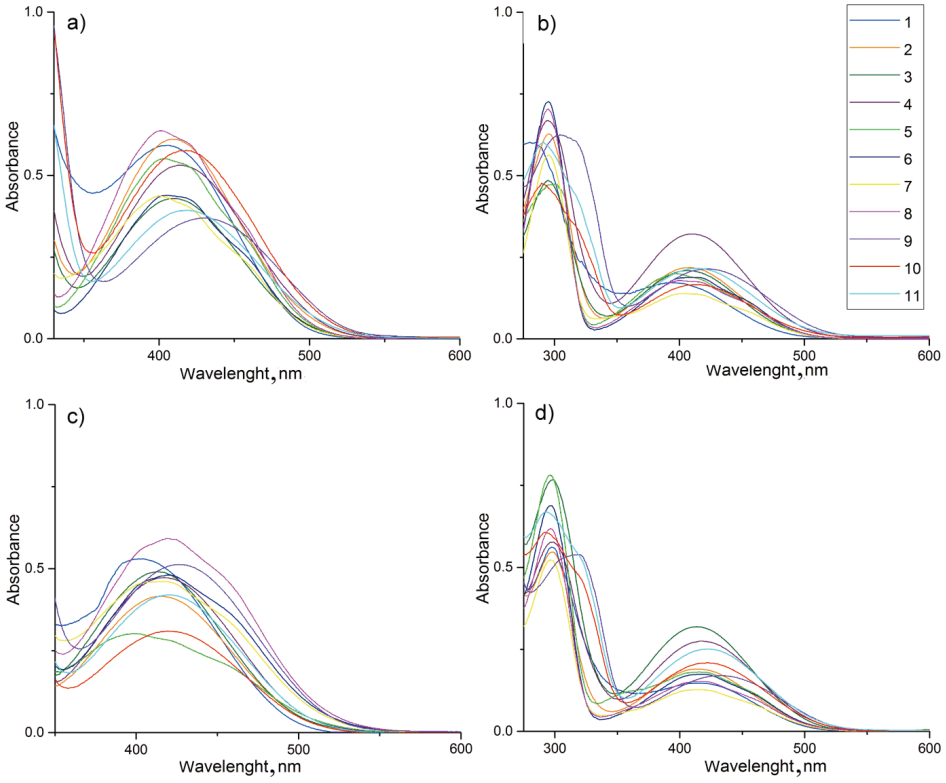

Fig. 2. UV–Vis absorption spectra of compounds **1**–**11** in: a) acetone, b) ACN, c) BnOH and d) DMF.

All UV–Vis spectra were recorded at concentration of 1×10^{-5} mol dm^{-3}, and the obtained data are presented in Tables II and S-III.

TABLE II. Absorption frequencies ($\nu_{max}\times10^{-3}$ / cm^{-1}) of isatin derivatives in selected solvents (higher wavelength peak)

Solvent	Compound										
	1	**2**	**3**	**4**	**5**	**6**	**7**	**8**	**9**	**10**	**11**
Methanol	–	26.95	24.21	–	26.81	–	29.37	24.01	23.58	24.1	24.01
Ethanol	24.48	24.18	24.27	24.1	26.67	26.39	21.57	24.15	23.39	24.04	24.18
2-Propanol	24.21	–	24.3	24.15	23.78	–	–	–	23.95	23.89	23.87
2-Butanol	23.95	24.3	24.39	23.92	26.11	23.89	24.94	23.92	23.31	23.81	23.89
Cyclohexanol	24.63	24.15	24.24	23.92	25.71	23.87	23.81	23.81	23.12	23.67	23.78
Benzyl alcohol	24.91	24.13	24.21	23.95	25.13	23.84	24.07	23.75	23.47	23.84	23.84
2-Methoxyethanol	–	24.18	24.13	23.98	26.67	26.92	–	24.24	–	23.92	23.98
2-Chloroethanol	–	–	25.58	23.92	23.98	23.95	23.95	23.98	25.51	24.3	26.63
DME	24.45	24.21	24.27	23.87	24.78	24.78	24.74	24.88	22.99	24.04	23.75
Toluene	24.04	24.51	24.21	23.58	24.88	24.81	24.88	24.91	22.91	–	23.42
DCM	24.21	24.18	24.45	23.98	24.84	23.95	24.69	23.92	23.72	24.13	23.95
Acetone	24.66	24.48	24.48	24.13	24.84	24.64	25.06	24.94	23.23	23.92	23.95
Cyclohexanone	24.51	24.07	24.3	23.84	25.71	24.45	24.81	24.78	22.91	23.75	23.67
EtOAc	24.54	24.57	24.24	23.98	25.06	24.94	24.97	24.84	23.12	23.81	23.78
Formamide	24.84	24.18	24.54	24.3	25.48	23.92	24.21	24.18	23.78	23.92	24.07
DMF	24.15	24.13	24.12	23.98	24.07	23.98	24.10	24.04	23.12	23.7	23.81
DMAc	23.98	23.92	23.96	23.87	23.89	23.78	23.87	23.81	23.04	23.81	23.56
NMP	23.70	24.04	23.92	23.75	23.81	23.72	24.01	23.81	22.88	23.61	24.21
ACN	25.41	24.51	24.66	24.42	25.28	24.3	24.69	25.00	23.72	24.27	23.78
DMSO	24.39	24.13	24.13	23.98	25.54	24.1	24.48	23.89	23.17	23.78	23.58
THF	23.95	24.3	24.15	23.89	25.13	24.69	24.75	24.81	22.96	23.58	23.64
2-Pyrrolidone	24.10	24.04	24.24	24.07	23.81	23.84	23.92	23.84	23.01	23.84	24.01

The shifts of ν_{max} in UV absorption spectra showed relatively weak dependences on both solvent and substituent effects (the observed change were in the range 10–20 nm) compared to those of the parent compound **1**. The data from Tables II and S-III indicate that the values of the absorption frequencies of the investigated compounds depended on the electronic effect of the substituent present at the C3 position of the indol-2-one core. The introduction of Br as a substituent at C4 of the phenyl ring (compound **4**) and all quinoline derivatives (compounds **9**–**11**) contributed to a positive solvatochromism, compared to the unsubstituted compound. The other compounds showed alternation of ν_{max}, shifting to higher wavelengths in 2-chloroethanol, 2-methoxyethanol, DMF, DMAc and ACN while in the other solvent, no regularity could be observed (irregular behaviour with respect to both substituent and solvent). Highest bathochromic shifts were found for compound **9** in almost all the solvent used.

Solvent effects on the UV–Vis absorption spectra: correlation with multi-parameter solvent polarity scales

The UV–Vis absorption spectra of the investigated isatin derivatives **1**–**11** were measured at 25 °C in twenty two solvents in the range 200–600 nm (Tables

II and S-III). The UV–Vis spectra consisted of two peaks which corresponded to different electronic transitions.

The Kamlet–Taft solvent parameters are taken from the literature[16] as well as substituent constants used in the LSER and LFER correlations.[11] To explain solvent and substituent effects on the electronic absorption spectra of the isatin derivatives, the absorption maxima of the lower energy band of the unsubstituted compound **1** in cyclohexane were taken as the reference. The data in Tables II and S-III confirmed that the positions of the UV–Vis absorption frequencies depended on the nature of the solvent used and the substituent present on the aryl or phenyl ring present at the imino group of the isatin derivatives.

The effect of solvent dipolarity/polarizability and hydrogen bonding ability on the absorption maxima shift were interpreted applying the principles of linear solvation energy relationship (LSER) using the Kamlet–Taft solvatochromic Eq. (1).[8] The results are presented in Tables III and S-IV, and coefficients v_0, s, b and a fitted at the 95 % confidence level.

TABLE III. The results of the correlation analysis for the isatin derivatives (higher wavelength peak) according to Eq. (1)

Compd.	v_0	s	b	a	R^a	SD^b	F^c	$P_\pi{}^d$	$P_\beta{}^d$	$P_\alpha{}^d$	Solvent excluded from the correlation
	$\times10^{-3}$ cm^{-1}										
1	25.31 ±0.23	0.27 ±0.20	–2.15 ±0.26	0.62 ±0.12	0.95	0.14	25.17	8.88	70.72	20.39	2-Chloroethanol, 2-methoxyethanol, DCM, cyclohexanol, toluene, DMSO, ACN, THF
2	25.35 ±0.12	–0.64 ±0.10	–1.02 ±0.13	–0.05 ±0.06	0.96	0.07	31.47	37.43	59.65	2.92	2-Propanol, 2-chloroethanol, 2-ethoxyethanol, DME, DCM, DMSO, toluene
3	24.62 ±0.10	0.77 ±0.13	–1.76 ±0.12	1.16 ±0.06	0.99	0.07	158.8	20.87	47.70	31.44	2-Chloroethanol, ethanol, BnOH, 2-methoxyethanol, formamide, toluene, DCM
4	23.70 ±0.08	0.32 ±0.08	–0.06 ±0.08	0.40 ±0.05	0.94	0.05	21.81	41.03	7.69	51.28	2-Chloroethanol, ACN, acetone, BnOH, 2-chloroethanol, EtOAc, NMP, 2-methoxyethanol, toluene, cyclohexanol

TABLE III. Continued

Compd.	ν_0	s	b	a	R[a]	SD[b]	F[c]	P_π[d]	P_β[d]	P_α[d]	Solvent excluded from the correlation
	$\times 10^{-3}$ cm^{-1}										
5	23.14 ±0.44	4.36 ±0.54	1.64 ±0.41	0.14 ±0.29	0.95	0.29	33.31	71.01	26.71	2.28	2-Chloroethanol, DMSO, BnOH, toluene, formamide, cyclohexanone, 2-methoxyethanol
6	26.03 ±0.20	–1.01 ±0.19	–1.57 ±0.24	–0.62 ±0.10	0.95	0.15	34.00	31.56	49.06	19.38	2-Chloroethanol, 2-propanol, ethanol, DCM, 2-methoxyethanol
7	26.24 ±0.22	–0.64 ±0.23	–2.14 ±0.28	–0.62 ±0.11	0.96	0.15	34.68	18.82	62.94	18.24	2-Propanol, 2-methoxyethanol, 2-chloroethanol, ethanol, 2-butanol, DMSO, toluene, DCM
8	26.54 ±0.23	–0.97 ±0.22	–2.28 ±0.27	–0.61 ±0.11	0.95	0.16	43.10	25.13	59.07	15.80	2-Propanol, 2-methoxyethanol, DCM, toluene, ethanol
9	22.44 ±0.33	1.64 ±0.44	–1.22 ±0.29	2.10 ±0.23	0.94	0.25	31.55	33.06	24.60	42.34	2-Methoxyethanol, 2-chloroethanol, ethanol, BnOH, formamide, 2-pyrrolidone
10	23.75 ±0.12	0.49 ±0.14	–0.65 ±0.10	0.53 ±0.06	0.94	0.07	32.38	29.34	38.92	31.74	Toluene, ACN, BnOH, formamide, 2-methoxyethanol
10	23.79 ±0.11	0.45 ±0.12	–0.69 ±0.09	0.54 ±0.06	0.96	0.07	42.18	26.79	41.07	32.14	Toluene, ACN, BnOH, formamide, 2-methoxyethanol, DME
11	23.00 ±0.41	1.62 ±0.63	–1.03 ±0.41	2.42 ±0.30	0.94	0.31	25.22	31.95	20.32	47.73	2-Chloroethanol, BnOH, formamide, DCM, ethanol, 2-pyrrolidone, 2-propanol, cyclohexanol

[a]Correlation coefficient; [b]standard deviation; [c]Fisher test of significance; [d]the percentage contribution of solvatochromic parameters obtained using the Kamlet–Taft Equation (%)

The correlation results obtained using the Kamlet–Taft Equation indicated that complex relation/alternation of solvatochromic coefficients with respect to solvent/substituent effects exists (Table III). The positive sign of the *s* and *a* coef-

ficients for isatin derivatives (compounds. **1**, **3**–**5** and **9**–**11**) indicate hypsochromic shifts with increasing solvent dipolarity/polarizability and hydrogen-bond donor capability. The largest hypsochromic shifts of the absorption maxima regarding the coefficients *s* and *a* were found for compounds **5** and **9**, respectively. The positive values of *s* and *a* coefficients suggest better stabilization of the ground state relative to the electronic excited state with increasing solvent polarity, *i.e.*, higher dipolar properties of the molecule in the ground state with more pronounced HBA properties of solvated molecules. The contrary is true for the other compounds. Considering the HBA solvent effect, the negative value of coefficient *b*, except compound **5**, indicated better stabilization of the excited state by solvent hydrogen bond accepting interactions.

The percentage contribution of solvatochromic parameters (Table III) for all isatin derivatives showed that compound **5** exhibited the highest P_π value (71.01 %) and the lowest P_α value (2.28 %). The opposite was observed for compound **1** that exhibited the highest value for P_β (70.72 %) and the lowest P_π value (8.88 %). Highest P_α value was obtained for compound **4** (51.28 %).

According to the correlation analysis obtained using the Kamlet–Taft Equation, the *s* and *a* coefficients were negative (Table S-IV), except for compound **9** (positive values of 1.57 and 1.42, respectively, were obtained), indicating a bathochromic shift with increasing solvent dipolarity/polarizability.

This suggests better stabilization of the electronic excited state relative to the ground state, *i.e.*, higher dipolarity/polarizability and HBD properties of the solvated molecules in the excited state. Alternation of the sign of the coefficients *b*, the positive values found for compounds **3**, **4**, **8** and **11** indicated better stabilization of the isatin derivatives in the ground state, *i.e.*, a higher HBA solvent interaction with solute molecule was found. For the other compounds, the opposite behaviour was found.

The non-specific solvent effect is the factor that contributes the most to the UV–Vis spectral shifts of all the investigated compounds (Table S-IV), except for compound **9**, for which the HBA solvent effect contributes the most (45.04 %), and compound **11**, for which P_α has the highest contribution (44.15 %). The highest value of P_π was obtained for compound **5** (65.41 %). The HBA of a solvent is of lower importance. The highest value of the solvent HBA effect was found for compound **9** (–2.45) and exceptionally low values were found for compounds **6**–**8** (–0.05, –0.06 and 0.02, respectively). The presented results obtained from the Kamlet–Taft model, indicate that the solvent effects on the change of the UV–Vis absorption spectra of the investigated isatin derivatives are very complex due to the diversity of the contribution of both solvent and substituent effects in the studied compounds. This also indicated that the electronic behaviour of the nitrogen atoms of indol-2-one moiety is significantly different between the deri-

vatives with a high contribution of a localized HBA effect caused and enhanced by electron-accepting quinoline and methyl substituted pyridyl groups.

Substituent effects on the NMR and UV absorption data: LFER analysis

The LFER concept was applied to the ν_{max} and *SCS* values of the isatin derivatives with the aim of obtaining an insight into the electronic effects of the substituents on the shifts in the absorption maxima and NMR chemical shifts. An analysis using LFER principles in the form of the Hammett Equation was performed.[9] The Hammett substituent constants are given in Table S-V, and the obtained correlation results are presented in Table IV. The observed ρ values indicate different susceptibilities of the chemical shifts to substituent effects. From Table IV it could be seen that the correlations are of good to high quality, which means that the *SCS* values reflect the electronic substituent effects. It is apparent that chemical shifts of C1′ showed an increased susceptibility and normal substituent effect.

TABLE IV. Correlation results of the *SCS* with the σ constants according to the Hammett (SSP) Equation

Atom	ρ	*h*	*R*	*F*	*SD*	*n*	Substituents included
H	–0.26 ±0.05	11.22 ±0.03	0.957	32.84	0.004	5	CN[a], 3-Me-2-pyridyl, 4-Me-2--pyridyl, 5-Me-2-pyridyl, 6-quinolinyl
	–0.34 ±0.05	11.26 ±0.03	0.971	49	0.004	5	3-Me-2-pyridyl, 4-Me-2-pyridyl, 5-Me-2-pyridyl, 6-Me-2-pyridyl, 6-quinolinyl
	–2.02 ±0.17	12.40 ±0.12	0.993	145.34	0.016	4	NO_2[a], CN, 4-Me-2-pyridyl, 6-Me-2-pyridyl
C2	–1.09 ±0.17	164.30 ±0.09	0.952	39.13	0.105	6	H, Br, 3-Br, CN, 5-Me-2-pyridyl, 6-Me-2-pyridyl
	–5.68 ±0.95	167.32 ±0.61	0.960	35.65	0.089	5	CN, 2-Br, 4-Me-2-pyridyl, 6-Me-2-pyridyl, 6-quinolinyl
C3	0.83 ±0.09	151.82 ±0.05	0.974	36.62	0.019	4	2-Br, 3-Br, 3-Me-2-pyridyl, 6-Me-2-pyridyl
C1′	19.74 ±3.00	142.05 ±1.76	0.957	43.28	1.392	6	Br, 3-Br, NO_2, 4-Me-2-pyridyl, 5-Me-2-pyridyl, 6-Me-2-pyridyl
	17.39 ±1.53	143.86 ±0.95	0.989	129.71	0.651	5	Br, NO_2, 4-Me-2-pyridyl, 5-Me-2-pyridyl, 6-Me-2-pyridyl
	6.02 ±1.12	151.70 ±0.69	0.952	28.76	0.701	5	H, NO_2, 4-Me-2-pyridyl, 5-Me--2-pyridyl, 6-Me-2-pyridyl

[a]NMR data for 4-NO_2 and 4-CN are taken from the literature[2]

The presented results indicate that the contribution of both substituent effects, electron-donating and electron-accepting, have significant influences on the electron-density shift in the overall investigated molecule. The effectiveness of the transmission of substituent effects is determined by the conformational

(geometry) change of the investigated molecules that originates from an out-of-plane rotation of the aryl substituent with respect to the indol-2-one plane, which is defined by the torsion angle θ (Fig. 1). The reverse substituent effect was observed at H1 and C2.

The existence of these correlations was interpreted as evidence for the effects of the substituents on the change in the electronic density over the investigated molecule. The presence of an electron-accepting keto group at the C2 position (C2=O) and an electro-donating amino group (N1–H), as a part of π_1-electronic system of amide group, contribute to intensive electronic interactions that exist in the 3-(substituted imino)-2-pyrrolidone moiety.[17] Correlations for C2 showed negative values of the correlation coefficients ρ. The negative sign of reaction constant, ρ, indicates the reverse behaviour, *i.e.*, the values of *SCS* decrease although the electron-withdrawing ability of the substituents, measured by σ, increase. Such findings clearly reflect the opposite behaviour to normal polarization in the keto group, which arises from the contributions of two opposing effects: the electron-accepting C2=O group and the aryl substituents with participation of an electron-donating effect of the indole nitrogen. The magnitude of this effect strongly depends on the electron-accepting character of aryl substituents, which cause an adequate/proportional reverse π-electron density shift from the C2=O keto group. The contribution of resonance interactions depends on the spatial arrangement of the aryl moiety and thus, a favourable conformation provides effective transmission of the resonance effect to the C2 and C3 carbons. According to this, it is expected that the presence of electron-donating group support normal polarization of C2=O and electron-accepting group exert the opposing effect, which is reflected in reverse polarization. Normal polarization at C3 carbon is a reflection of the contribution of electronic effects in both π-electronic units (Fig. 1) and is primarily dictated by the polarization of the C=N imino bond, which is more or less disturbed by a change of the substituent at the phenyl (aryl) moiety. It is obvious that the chemical shifts of C1′ show an increased susceptibility and normal substituent effect in relation to the substituent constant. This finding appears as a consequence of short-range electronic interaction with a substituent in the *para*-position of the phenyl ring.

The correlation results for the UV–Vis absorption maxima of the investigated compounds, obtained by the use of LFER principles, are given in Table V. The LFER results indicate the complex influences of both solvent and the substituent effect on the shifts of the UV–Vis absorption maxima (Table V).

These results indicate that solvent effects: dipolarity/polarizability, HBD and HBA abilities cause appropriate sensitivity of the position of the absorption maxima (ν_{max}) to the substituent effect.

The highly dipolar aprotic solvent, DMF, and the solvent with a low HBD effect, ACN, and high HBD effect, ethanol, contribute to the opposing behaviour

of the shift in the absorption frequencies at the higher wavelength with respect to the substituent effects. Aprotic solvents behave as poor anion solvators, while they usually stabilize better larger and more dispersible positive charges. Lower contribution of substituent effects in solvent with higher relative permittivity could be explained by the fact that highly dipolar surrounding medium suppresses electron density shift inducing lower susceptibility of the absorption maxima shift to electronic substituent effects. Similar behaviours were found for ACN and ethanol, and it could be observed that solvent dipolarity/polarizability is the most significant effect that contributes to the reverse relationship of ν_{max} to substituent effects. An opposite substituent effect on ν_{max} change was found in THF.

TABLE V. Correlation results of the ν_{max} values with σ substituent constants using the Hammett (SSP) Equation

Atom	Solvent	ρ	h	R	F	SD	n	Substituents included
Peak at lower wavelength	DMF	0.90 ±0.18	33.08 ±0.11	0.961	24.48	0.043	4	2-Br, 3-Br, 4-Me-2-pyridyl, 6-Me-2-pyridyl
	Ethanol	0.47 ±0.08	33.05 ±0.05	0.958	33.33	0.030	5	2-Br, 4-Br, 4-Me-2-pyridyl, 5-Me-2-pyridyl, 6-Me-2-pyridyl
		0.35 ±0.06	33.14 ±0.03	0.961	35.92	0.036	5	H, 4-Br, 4-Me-2-pyridyl, 5-Me--2-pyridyl, 6-Me-2-pyridyl
	ACN	–3.19 ±0.31	35.90 ±0.17	0.981	102.97	0.180	6	H, 2-Br, 4-Me-2-pyridyl, 5-Me--2-pyridyl, 6-Me-2-pyridyl, 8-OH-2-quinolinyl
		–0.25 ±0.03	34.06 ±0.02	0.976	60.90	0.012	5	3-Br, 4-Br, 4-Me-2-pyridyl, 5-Me-2-pyridyl, 6-Me-2-pyridyl
	THF	1.12 ±0.15	33.37 ±0.08	0.975	57.52	0.058	5	3-Br, 4-Br, 4-Me-2-pyridyl, 5-Me-2-pyridyl, 6-Me-2-pyridyl
Peak at higher wavelength	DMF	–1.31 ±0.24	24.88 ±0.15	0.967	28.80	0.020	4	2-Br, 3-Me-2-pyridyl, 4-Me-2-pyridyl, 5-Me-2-pyridyl
		–0.82 ±0.12	24.15 ±0.05	0.979	45.04	0.056	4	H, 4-Br, 6-quinolinyl, 8-OH-2-quinolinyl
	Ethanol	–0.51 ±0.06	24.47 ±0.03	0.977	62.21	0.033	5	H, 2-Br, 3-Br, 6-Me-2-pyridyl, 8-OH-2-quinolinyl
	ACN	–1.67 ±0.18	25.38 ±0.09	0.982	82.97	0.100	6	H, 2-Br, 3-Br, 4-Me-2-pyridyl, 8-OH-2-quinolinyl, 6-quinolinyl
	THF	2.03 ±0.29	23.42 ±0.16	0.971	48.85	0.115	5	3-Br, 4-Br, 4-Me-2-pyridyl, 5-Me-2-pyridyl, 6-Me-2-pyridyl

In the two solvents that show HBD properties, ACN and ethanol, a negative correlation slope of the lower wavelength peak was obtained for the former solvent. A somewhat higher sensitivity of ν_{max} to the substituent effect was found for ACN (first set of solvents), and THF. In DMF, ethanol and THF, negative solvatochromism was obtained with respect to the substituent effects, which indicates better stabilization of ground state of the investigated compounds. Some-

what lower values and similar trend of the correlation slope was found for ethanol, due to lower contribution of solvent dipolarity/polarizabilty effect. This result suggests that the transmission of the electronic substituent effects significantly depends on the conformation of studied molecules and solvent properties. Presented results showed that transmission of substituent electronic effects through π-resonance units occurs by a balanced contribution of two modes: through the localized π-electronic unit and the overall conjugated system of the investigated compounds. Their contribution depends on the substitution pattern, as well as on the solvent properties. This fact implies that electron density change is based on the localized/extended delocalization phenomena for the electron-acceptor substituted compounds. The consequence is the lower substituent effect in a solvent with higher hydrogen bond accepting ability.

Optimized geometries and MEP *analysis of the investigated compounds*

An additional analysis of solvent and substituent effects on the absorption frequencies and conformational changes of the studied compounds necessitated theoretical calculations, *i.e*., geometry optimization and *MEP* analysis. Geometry optimization of the investigated molecules was performed by using the B3LYP functional with the 6-311G(d,p) basis set. The most stable conformations of compounds **1**–**11** are presented in Fig. 3. Elements of the optimized geometries of the calculated compounds are given in Table VI. The theoretical absorption spectra of compound **1** (data shown in the Supplementary material, Table S-VI) were calculated in acetone, acetonitrile, ethanol, tetrahydrofuran, dimethyl sulfoxide, formamide and toluene by the TD-DFT method, and showed very good agreement with the experimental data.

The calculation of the optimal geometry, with focus on the determination of the value of the torsion angle θ (Fig. 1), gives valuable results required for a better understanding of the transmission of substituent effects, *i.e*., the electron density distribution. A more planar molecule, *i.e*., a molecule with a smaller torsional angle, induces a red shift in the absorption spectra.[18,19] In the investigated molecules, the values of θ are different and mostly depend on the substituent present. Somewhat larger deviations of θ were registered for compounds **2**, **5**–**8** and **11** (Table VI), indicating the significance of extended resonance interaction in electron-donor substituted compounds. On the contrary, in electron-acceptor substituted compounds, an appropriate contribution of n,π-conjugation (nitrogen lone pair participation) to overall electronic interaction with the π-electronic system of the pyridone unit causes perturbation of the π-electron density.

The elements for the geometries of the substituted isatin derivatives are similar to those for the unsubstituted one. The introduction of a mainly electron-accepting substituent causes a decrease in the C3=N bond length, *i.e*., the substituent supports the normal polarization in the imino group resulting in an appro-

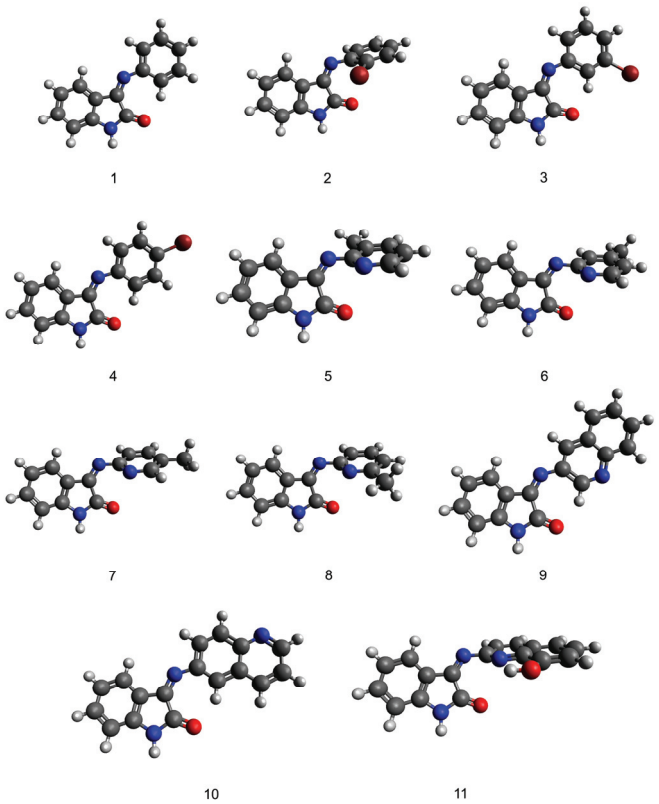

Fig. 3. Optimized geometry of the investigated compounds.

TABLE VI. Optimized geometry parameters obtained in DFT calculations

Compd.	Interatomic distance, Å					Torsional angle[a]
	N1–C2	C2=O	C2–C3	C3=N	N–C1′	θ / °
1	1.3830	1.2208	1.5451	1.2849	1.3931	0.021
2	1.3857	1.2125	1.5449	1.2751	1.4053	69.686
3	1.3819	1.2202	1.5464	1.2845	1.3933	0.045
4	1.3820	1.2210	1.5451	1.2854	1.3913	0.006
5	1.3889	1.2120	1.5464	1.2762	1.4058	60.636
6	1.3888	1.2120	1.5469	1.2757	1.4062	61.201
7	1.3892	1.2121	1.5469	1.2769	1.4046	58.482
8	1.3890	1.2121	1.5472	1.2762	1.4056	59.411
9	1.3827	1.2195	1.5462	1.2854	1.3889	0.179
10	1.3818	1.2216	1.5446	1.2856	1.3917	0.029
11	1.3876	1.2122	1.5480	1.2770	1.4018	60.877

[a]Torsional angle between the isatin and aryl planes

priate shift of the electron density to nitrogen. The presence of an electron-donating group attached at the complex structure of the aryl moiety contributes to an

electron density shift from the phenyl ring to the indole moiety resulting in an increased molecule planarization. A decrease of the C2=O lengths is caused by the superposition of two effects: normal polarization in the C2=O bond and the opposing effect of an electron-withdrawing group at the C3 position, which results in a slight shifting of the π-electron density to the carbonyl carbon. As a consequence, the length of the N1–C2 bond increases, compared to that in compound **1** as a result of the suppression of amide type of resonance.

A larger deviation from planarity was found for compounds **2**, **7**, **8** and **11**, which is associated with the *ortho*-effect of 2-Br in **2**, the presence of an electron-donating methyl group situated in different position at the pyridyl (**7** and **8**) and a strongly electron-donating hydroxyl group in **11**. Two opposing electron accepting effects are operative in the investigated compounds: electron-accepting aryl substituents and the indol-2-one core, which influence appropriate geometrical adjustment of these molecules as a response to the electronic demand of the electron deficient environment, except in the vicinity of the electron density at C2=O and the nitrogen atom in compounds **5**–**8** and **11**, which are also contributing factors to increased deviation from planarity due to repulsion of the negative potential present at these molecular fragments.

The variation of substituent patterns clearly indicates that contributions of both conformational arrangement and donor-accepting character are involved in the electronic transitions of the investigated compounds. In addition, the electron density of the investigated compounds is investigated using *MEP* analysis, which enabled the visualization of the electron density distribution for the studied compounds. *MEP* analysis was used to evaluate and visualize the charge distribution over the investigated molecules and illustrates the three-dimensional charge distributions over all the molecules. The *MEP* at a point in space around a molecule gives information about the net electrostatic effect produced at that point by the total charge distribution (electron + proton) of the molecule and correlates with dipole moments, electronegativity, partial charges and chemical reactivity of the molecules. It provides a visual method to understand the relative polarity of the molecule.[20,21] An electron density isosurface mapped with electrostatic potential surface depicts the size, shape, charge density and site of chemical reactivity of molecules. The *MEP* profiles shown in Fig. 4 illustrate the three-dimensional charge distributions over all the investigated molecules. As can be seen from Fig. 4, different values of the electrostatic potential at the surface are represented by different colours; red represents regions of the most electronegative electrostatic potential, it indicates the region of high electron density, *i.e.*, sites favourable for electrophilic attack; blue represents regions of the most positive electrostatic potential, *i.e.*, regions of low electron density favourable for nucleophilic attack, and green represents regions of zero potential. Potential increases in the order red < orange < yellow < green < blue. The blue colour indicates a strong attract-

ive potential, a region favourable for HBA solvent interaction, while the red colour indicates repulsive potentials, and includes sites favourable for HBD solvent interactions.

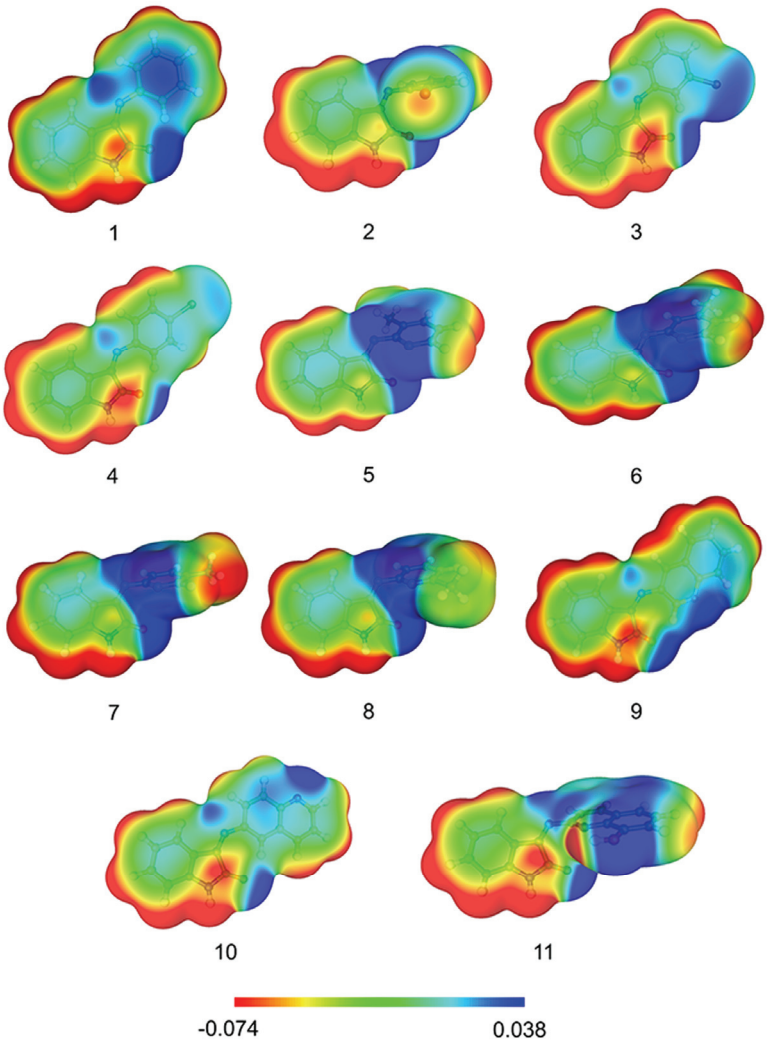

Fig. 4. *MEP* maps of the investigated compounds.

There is an obvious negative potential at the oxygen atom, a part of the keto group (C2=O) in the indol-2-one structure, and nitrogen atom present in the structure of the aryl substituent. Thus, most of the HBA capabilities of investigated compounds could be assumed to be from the keto group (C2=O) and the aryl nitrogen, which are electron-acceptor groups and cause an increase in the

electron densities at these two sites, providing for favourable interactions with proton-donating solvents.

In the molecules that contain heterocyclic structure with nitrogen atom an increase in the electron density is noticeable, which acts as a centre that showed significant proton-acceptor interaction with solvent molecules (increased HBD effect).

Non-planarity of investigated molecule significantly contributes to the electron density distribution and electron density transfer that occurs due to the both solvents and substituent influence. It is particularly interesting to note that apart from the inductive effect, resonance effect of nitrogen atom plays an important role in increasing the substituents' negative potential which causes significant contribution of HBD solvent effect. In cases where nitrogen heteroatoms are in the *ortho* position relative to the C=N bond (compounds **5**–**8** and **11**) steric hindrance is observed, and increase in the electron density of nitrogen as a result of obtained conformation of the investigated compound which results in reduction of the electron density in the rest of the heterocyclic ring. These factors contribute to an increasing of the proton-accepting capability with solvent molecules that have a pronounced HBD effect.

The influence of the position of a substituent on the electronic effects was investigated and different geometries and electron density distributions were observed using compounds **2**–**4** as examples. The effect of a bromine atom, which shows a negative inductive and a positive resonance effect on the electron density distribution over the compounds **2**–**4** significantly depends on the substituent position, *i.e.*, *ortho*, *meta* or *para*-position. The electron-acceptor effect of the bromine atom induces the shifting of the electron density, which results in the significant change in the geometry of the ortho, meta and para-derivatives. It consequently contributes to the difference in the electron density distribution and therefore to different interactions of the mentioned derivatives with the solvent which is used.

CONCLUSIONS

The UV–Vis and NMR data of eleven isatin derivatives, *i.e.*, Schiff bases, were analyzed using the LSER and LFER principles. The solvatochromism of the investigated compounds was analyzed with the Kamlet–Taft model. The positive sign of the *s* and *a* coefficients for compounds **1**, **3**–**5** and **9**–**11** (higher wavelength peak) indicates hypsochromic shifts. Considering HBA solvent effect, the negative value of coefficient *b*, except for that of compound **5**, indicated better stabilization of the excited state. On the contrary, the negative sign of the *s* and *a* coefficients, except for those of compound **9**, indicate a bathochromic shift of the lower wavelength peak with increasing solvent dipolarity/polarizability. Alter-

nation of the sign of coefficients *b*, positive values found for compounds **3**, **4**, **8** and **11** indicated better stabilization of the ground state.

The LFER analysis applied to the NMR chemical data and ν_{max} implies that solvent effects have a significant influence on the transmission mode of substituent effects. The LFER analysis of NMR data at H1 and C2 showed opposing behaviour, and the highest susceptibility to substituent effects was observed for C1′. Positive solvatochromism was found in THF, DMF and ethanol for the lower wavelength peak. Opposing behaviour was found in ACN.

Quantum chemical calculations showed that the present substituents significantly changed the extent of conjugation. The *MEP* maps show that regions with negative potential are over the electronegative oxygen atoms in C2=O and nitrogen present in pyridyl and quinolinyl ring at C3=N position. On the other hand, the region with a positive potential are over the phenyl and the rest of substituent rings showing mostly HBD capabilities. The theoretical calculations and experimental results gave an insight into the influence of the molecular conformation on the transmission of substituent effects, as well as on the contribution of different solvent–solute interactions.

SUPPLEMENTARY MATERIAL

General methodology for the preparation of isatin derivatives and characterization data are available electronically at the pages of journal website: http://www.shd.org.rs/JSCS/, or from the corresponding author on request.

Acknowledgements. The authors acknowledge the financial support of the Ministry of Education, Science and Technological development of the Republic of Serbia (Project No. 172013).

ИЗВОД

СОЛВАТОХРОМИЗАМ ШИФОВИХ БАЗА КОЈЕ СУ ДЕРИВАТИ ИЗАТИНА: LSER И LFER СТУДИЈА

ДОМИНИК Р. БРКИЋ[1], АЛЕКСАНДРА Р. БОЖИЋ[1], ВЕСНА Д. НИКОЛИЋ[2], АЛЕКСАНДАР Д. МАРИНКОВИЋ[3], HANA ELSHAFLU[3], ЈАСМИНА Б. НИКОЛИЋ[3] и САША Ж. ДРМАНИЋ[3]

[1]Београдска политехничка школа, Бранкова 17, 11000 Београд, [2]Хемијски факултет, Универзитет у Београду, Студентски трг 12–16, 11000 Београд и [3]Катедра за органску хемију, Технолошко–металуршки факултет Универзитета у Београду, Карнегијева 4, 11120 Београд

Деривати изатина су познати по томе што показују биолошку активност. Међутим, утицај растварача на њих није детаљиније испитиван досад, а могао би, поготово повезан са њховом електронском структуром, бити интересантан као део њихове карактеризације. Линеране корелације солватационих енергија (LSER) су примењене на утицај растварача на UV апсорпционе максимуме испитиваних Шифових база које су деривати изатина, помоћу Камлет–Тафтове једначине. Затим су линеране корелације слободних енергија (LFER) примењене на хемијска померања индукована супституентима (*SCS*), помоћу једнопараметарског метода (SSP). Показало се да присутни супституенти мењају електронску конјугацију и интрамолекулски пренос наелектрисања. Добијене корелације, заједно са теоријским прорачунима, дају увид у утицај молекулских конформација на пренос ефеката супституената, као и на интеракције између растварача и рас-

творене супстанце. Мапе површина молекулских електростатичких потенцијала (*MEP*) су приказане за оптимизоване геометрије молекула, да би се видео распоред електронских густина, који објашњава порекло интеракција између растварача и растворене супстанције.

(Примљено 19. јануара, ревидирано 20. априла, прихваћено 8. маја 2016)

REFERENCES

1. A. Medvedev, O. Buneeva, V. Glover, *Biologics* **1** (2007) 151
2. G. M. Šekularac, J. B. Nikolić, P. Petrović, B. Bugarski, B. Đurović, S. Ž. Drmanić, *J. Serb. Chem. Soc.* **79** (2014) 1347
3. R. W. Daisley, V. K. Shah, *J. Pharm. Sci*. **73** (1984) 407
4. E. Piscopo, M. V. Diurno, R. Gogliardi, M. Cucciniello, G. Veneruso, *Boll.-Soc. Ital. Biol. Sper*. **63** (1981) 827
5. S. N. Pandeya, D. Sriram, E. De. Clercq, C. Pannecouque, M. Witvrouw, *Indian J. Pharm. Sci*. **60** (1998) 207
6. V. A. Muthukumar, H. C. Nagaraj, D. Bhattacherjee, S. George, *Int. J. Pharm. Pharm. Sci*. **5** (Suppl. 3) (2013) 95
7. C. Reichardt, *Solvents and Solvent Effects in Organic Chemistry*, Wiley–VCH Verlag, Wienheim, 2004, p. 329
8. M. J. Kamlet, J. L. M. Abboud, R. W. Taft, *An examination of linear solvation energy relationships*, in *Progress in Physical Organic Chemistry*, Vol. 13, R. W. Taft, Ed., Wiley, New York, 1981, p. 485
9. L. P. Hammett, *J. Am. Chem. Soc*. **59** (1937) 96
10. O. Exner, in *Advances in Linear Free Energy Relationships*, N. B. Champan, J. Shorter, Eds., Plenum Press, London, 1972, p. 1
11. C. Hansch, A. Leo, D. Hoekman, *Exploring QSAR: Hydrophobic, Electronic and Steric Constants,* ACS Professional Reference Book, American Chemical Society, Washington DC, 1995
12. T. Yanai, D. Tew, N. Handy, *Chem. Phys. Lett.* **393** (2004) 51
13. J. Tomasi, B. Mennucci, R. Cammi, *Chem. Rev.* **105** (2005) 2999
14. Gaussian 09, revision C.02, Gaussian, Inc., Pittsburgh, PA, 2009
15. L. Laaksonen, *J. Mol. Graphics* **10** (1992) 33
16. M. J. Kamlet, J. L. M. Abboud, M. H. Abraham, R. W. Taft, *J. Org. Chem*. **48** (1983) 2877
17. F. H. Assaleh, A. D. Marinković, J. Nikolić, N. Ž. Prlainović, S. Drmanić, M. M. Khan, B. Ž. Jovanović, *Arabian J. Chem*. (2015) doi:10.1016/j.arabjc.2015.08.014
18. I. Ajaj, J. Markovski, M. Rančić, D. Mijin, M. Milčić, M. Jovanović, A. Marinković, *Spectrochim. Acta, A* **150** (2015) 575
19. I. Ajaj, J. Markovski, J. Marković, M. Jovanović, M. Milčić, F. Assaleh, A. Marinković, *Struct. Chem*. **25** (2014) 1257
20. S. Chidangil, M. K. Shukla, P. C. Mishra, *J. Mol. Model*. **4** (1998) 250
21. F. J. Luque, J. M. Lopez, M. Orozco, *Theor. Chem. Acc*. **103** (2000) 343.